water

MDPI

Article

Features of the Formation of Strontium Pollution of Drinking Groundwater and Associated Health Risks in the North-West of Russia

Alexander I. Malov

N. Laverov Federal Center for Integrated Arctic Research of the Ural Branch of the Russian Academy of Sciences, 20 Nikolsky Ave., Arkhangelsk 163020, Russia; malovai@yandex.ru

Abstract: The purpose of this research was to determine the natural factors that contribute to maintaining the standard quality of fresh drinking groundwater in areas with high strontium content. Hazard index values for the consumption of water containing strontium were also calculated to assess the overall non-carcinogenic health risk from combined ingestion and dermal exposure. The results showed that the groundwater with strontium concentrations exceeding the maximum permissible concentrations had an increased correlation of strontium concentrations with total dissolved solids and celestite and gypsum saturation indices. A decrease in calcium content was recorded with a simultaneous increase in the concentration of magnesium and strontium. Reducing conditions in the aquifer were also favorable for the conservation of these waters. In waters of standard quality, all these factors did not appear, which indicates their formation in sediments with discretely located small inclusions of celestite and gypsum. These waters were characterized by a calcium bicarbonate composition, low total dissolved solids (TDS), and oxidizing conditions. Elevated radiocarbon contents indicate their relatively young age. In general, it was found that children in the study area are most vulnerable to risks. Fifty percent of wells supply drinking water that is unsafe for consumption. The water from about a third of the wells studied is dangerous for adults.

Keywords: drinking water; Sr; isotope–chemical composition; dating; health risks

Citation: Malov, A.I. Features of the Formation of Strontium Pollution of Drinking Groundwater and Associated Health Risks in the North-West of Russia. *Water* **2023**, *15*, 3846. https://doi.org/10.3390/w15213846

Academic Editors: Weiying Feng, Fang Yang and Jing Liu

Received: 4 October 2023
Revised: 1 November 2023
Accepted: 1 November 2023
Published: 3 November 2023

1. Introduction

Groundwater is one of the main components of the environment, without which the existence of living organisms, including humans, is impossible. Groundwater has a number of significant advantages over surface water as it is better protected from environmental pollution than surface water and should be used first [1]. However, due to their dynamism, they actively participate in the processes of interaction between water and rocks, transferring various chemical elements into solution, including those that negatively affect the quality of drinking water [2–5].

The greatest difficulties are presented by elements whose maximum permissible concentrations (MPC) are characteristic of natural waters (e.g., in $mg \cdot L^{-1}$: Fe 0.3, F 1.2–1.5, Be 0.0002, Se 0.01, As 0.05, Sr 7.0, Mn 0.1) [6]. The low maximum permissible concentrations of these elements are explained by their organoleptic (Fe, Mn) and sanitary–toxicological properties (F, Be, Se, As, Sr).

According to [7], animal studies have shown that the chemical similarity of strontium to calcium allows it to be exchanged for calcium in various biological processes; the most important of these is the replacement of calcium in the bones, which affects skeletal development, causing changes similar to those associated with rickets [8–11]. Strontium may reduce cartilaginous bone calcification in children and adolescents with greater effects than those in adults [12].

The study of strontium in relation to diseases with a predominant lesion of the osteoarticular system in the form of deforming chondroosteoarthritis began more than 170 years

ago with Russian scientists' pioneering work on Urovskaya disease (the name was given according to the place of its first discovery: the Urov River near Lake Baikal in the south of Central Siberia) or Kashin–Beck disease (after the names of the doctors who first studied this disease) [13]. Later, it turned out that this disease is also common in Tadzhikistan [14], NW China [15], North Korea, and possibly in some areas of Africa [16,17]. However, despite a long period of study, the exact cause of this disease has not yet been established. Currently, more than 20 theories and hypotheses are being discussed in the scientific literature to explain the etiology and factors of the disease. The priority theory is biogeochemical, according to which the occurrence and course of the disease depend on environmental factors (i.e., a lack/excess of chemical elements or compounds). In particular, researchers have paid special attention to deficiencies of selenium and calcium and the low Ca:Sr ratio in groundwater and surface water, bottom sediments, soil, vegetation, animal bones, human teeth, and hair [18–21].

The relevance of studying fresh groundwater is due to the fact that: (1) drinking water is the most necessary and obligatory substance in the human diet, (2) groundwater with a high strontium content forms regional hydrogeochemical provinces in areas of widespread carbonate rocks in humid areas [11,22,23], and (3) groundwater with high strontium content is also widespread in arid zones due to the evaporative concentration of relatively shallow groundwater [2]. Significant research has been carried out in central Russia, Siberia, China, the US, and Australia [24–30]. Geological–hydrogeological, statistical, and thermodynamic analyses have shown that in a number of cases there is a relationship between the strontium content in water and the lithology of rocks, the age of groundwater, the total dissolved solids (TDS), and the degree of saturation of groundwater in relation to gypsum and celestite. However, the correlations were often somewhat weak [29].

In northwestern Russia, the highest Sr concentrations were established relatively recently in the carbonate aquifer in the mouth area of the Mezen River basin (see Figure 1b) [31]. Contamination of groundwater with strontium was also confirmed when drilling wells for water to the south in the cities of Karpogory, Bereznik, Shenkursk, and Velsk (see Figure 1a), and the implementation of a joint project by geochemists from Russia, Finland, and Norway, showed that over the entire area of distribution of Permian rocks P_1s, P_2u, P_2kz, and P_2t (see Figure 1a), even the surface water contains strontium at a level of 0.5 to 2 mg·L^{-1} [32].

However, it remains unclear why there is a significant variation in strontium concentrations in groundwater over short distances. At the same time, in our opinion, it is obvious that the conditions for the formation of groundwater with high and low strontium concentrations are different, and it is necessary to look for correlation dependencies separately for these two types of groundwater. Due to the fact that the MPC of strontium in Russia is 7 mg·L^{-1}, this value was chosen during the study to separate two groundwater clusters. The statistical study also showed that there is indeed a bimodal distribution of Sr concentrations in water, with the above two clusters being identified (see Figure S1, Table S1, and Section S1 of the Supplementary Materials). The Shapiro–Wilk test of normality indicated that there is a possibility of normal distributions in these two clusters (Table S2).

The purpose of this research was to determine natural factors that contribute to maintaining the standard quality of fresh drinking groundwater in areas where high strontium concentrations occur. To assess the overall non-carcinogenic health risk from combined ingestion and dermal exposure, hazard index (HI) values from consumption of water containing strontium were also calculated (see Section S4 of Supplementary Materials). Values below one indicate no significant non-cancer health risk. HI values greater than one reflect the potential for non-cancerous health outcomes, and this probability increases as HI values rise [33].

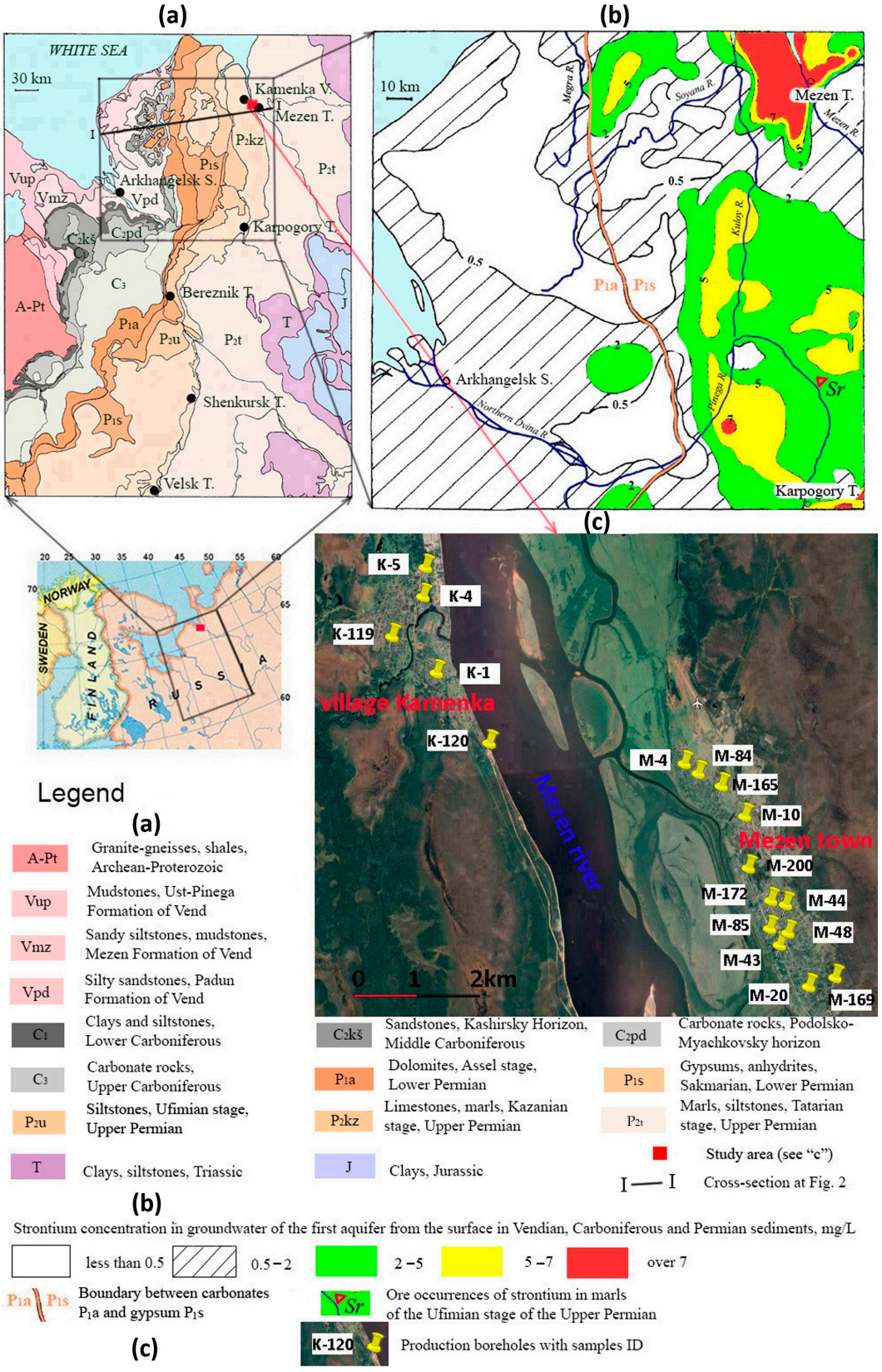

Figure 1. General location of the study site showing (**a**) geology, (**b**) strontium distribution in groundwater of the first aquifer from the surface (after [31]), and (**c**) sampling locations. I—I—cross-section at Figure 2.

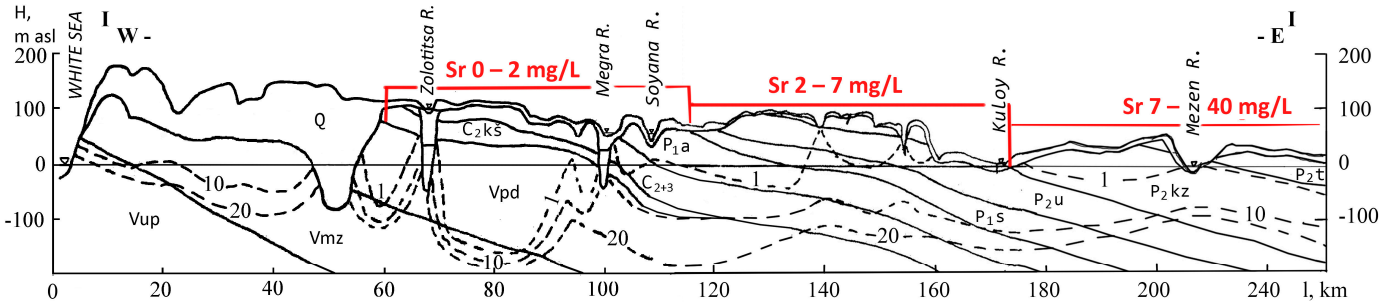

Figure 2. Schematic hydrogeological section along line I–I in Figure 1a. The dotted lines show the isolines of the total mineralization of groundwater (according to [31]); the red color shows the concentrations of strontium in fresh groundwater. Designations in Figure 1.

2. Geological Conditions

The research area is located in the junction zone of the Mezen syneclise and the eastern slope of the Baltic shield. Figure 1a shows the outcrop of this shield, composed of the most ancient Archean–Early Proterozoic (A-Pt) primary sedimentary rocks, transformed into intensely deformed and deeply metamorphosed gneisses, granite gneisses, amphibolites, and crystalline schists. At the beginning of the Riphean period (R) of the Late Proterozoic stage, a system of narrow extended grabens (aulacogens) was formed in this crystalline basement, which was filled with terrigenous, carbonate–terrigenous, and effusive-terrigenous strata up to several kilometers thick. Regional subsidence of the territory, which is associated with the formation of the Mezen syneclise, began in the Vendian (Ediacaran) period of the Late Proterozoic.

Sedimentation of the Ust Pinega (Vup) and Mezen (Vmz) formations (see Figure 2) proceeded in a relatively shallow epicontinental sea with weak hydrodynamics and a predominance of a reducing geochemical setting. Thin horizontal layering of the band type, accentuated by films of organic matter, probably arose during seasonal climate fluctuations. Against the background of calm and unidirectional subsidence, at times there were short-term rises of the bottom, accompanied by shallowing of the sea, as evidenced by the appearance of thin layers of siltstones and sandstones in the section. The formation of coarse-grained facies (probably deltaic or coastal-marine) in the Padun Formation (Vpd) is associated with the activation of multidirectional tectonic movements. From the end of the Vendian to the beginning of the formation of the Lower Carboniferous deposits, the region was mainly an area of removal and continental weathering. The significant proportion of kaolinite and cement in the terrigenous formations of the Vendian Padun Formation testifies to intense weathering processes [34,35].

In the Lower Carboniferous (C_1), the subsidence of the territory begins. The sediments are dominated by clays and siltstones, with interlayers of sandstones and conglomerates and thin interlayers of carbonate rocks: dolomites, limestones, and marls. The facies variability of the rocks of the Kashir horizon of the Middle Carboniferous (C_2kš), the absence of irregularities in the distribution of clastic material in terms of granulometric composition, poor roundness, and sorting of fragments, the presence of layers of gravelstones and conglomerates, and a sharp variability in thickness indicate the accumulation of these deposits in a turbulent coastal environment. The maximum distribution of the Middle Carboniferous Sea occurred during the Podolian time (C_2pd). Large areas accumulated dolomites and limestones. The fauna from these deposits testifies to a shallow, coastal zone of the marine basin with a salinity close to normal. In the Upper Carboniferous (C_3), the transgression reaches its maximum size. At this time, thick strata of dolomites had accumulated over most of the area.

The beginning of the Permian period was marked by a powerful Asselian transgression (P_1a), which manifested itself on a planetary scale. The marine basin was characterized by normal salinity and mostly shallow water, which is confirmed by the diversity of faunal remains. However, in some areas there was a regime in which the conditions of

sediment deposition somewhat deviated from those of a normal sea basin, and here lagoons periodically formed, which are associated with the appearance of gypsum interlayers. The salinization and regression of the sea, which began in the Upper Asselian, continued most intensively in the Sakmarian time (P_1s), by the end of which the territory was a gradually salinizing lagoon. Here, at first, the accumulation of dolomites containing gypsum interlayers occurred, followed by the accumulation of thick strata (about 80 m) of gypsum and anhydrites.

The type of sediments of the Ufimian stage of the Upper Permian (P_2u), represented mainly by red-colored siltstones, indicates that their accumulation occurred in a lagoonal–continental setting under arid climate conditions. The gypsum content of the rocks is replaced by celestite ore occurrences in the direction from the base to the top of the formation (see Figure 1b). The accumulation of sediments of the Kazanian stage of the Upper Permian (P_2kz) is associated with successive transgressions of the sea and its regression. Therefore, marls and calcareous clays are replaced by clayey, sandy, and dolomitic limestones with inclusions of gypsum and anhydrite. The Tatarian stage (P_2t) is represented at the base of the section by marls and siltstones with horizontal or similar bedding, which indicates the existence of a basin whose conditions were close to marine ones. Subsequently, there was an increasing desalination of the saline lagoons with the formation of the sandy–silty part of the sediments.

This regime did not last long. Subsequently, the entire territory entered the path of the predominantly continental Mesozoic–Cenozoic stage of denudation leveling. During this period, a significant part of the Lower Permian gypsum anhydrite sequence, distributed at least 100–150 km west of the currently observed boundary of the Sakmarian stage of the Lower Permian, was eroded (see Figures 1 and 2) [31].

As shown in Figure 2, the maximum concentrations of strontium, at 7–40 mg·L^{-1}, in fresh groundwater are confined to the distribution area of the Kazanian-stage carbonate deposits. To the west, in the area of accumulation of thick strata of gypsum and anhydrites, they decrease to 2–7 mg·L^{-1}, and further to the west, terrigenous-carbonate rocks contain groundwater with minimal concentrations of strontium. In [31], it is shown that, in general, one can note the dependence of the strontium content in water on its concentrations in rocks: in the direction from east to west they decrease from 2400 to 10 mg·kg^{-1}. The Sr content in sandstones is 200 mg·kg^{-1}, and in carbonate rocks is 610 mg·kg^{-1} [36,37].

The waters with the highest concentrations of strontium are the most dangerous for consumption, since in addition to the strontium content above the MPC for fresh drinking water, Ca/Sr << 100 ratios are also observed, which can cause the occurrence of Urov endemia (Kashin–Beck disease) [2].

3. Materials and Methods

In June 2022, 17 samples of drinking water used for water supply to the population were taken from boreholes located in the estuary zone of the Mezen River basin (see Figure 1c) for the purpose of studying the isotopic chemical composition (see Tables 1–3). The field sample preparation was carried out as described in a previous paper [38]. The analytical procedures are also described in previous papers [38,39]. The calcium, strontium, magnesium, sodium, and potassium concentrations were determined with an uncertainty degree of 1–2% by using an atomic absorption spectrometer (AAS) (Perkin-Elmer 5100 PC, Turku, Finland). Alkalinity was measured by potentiometric titration with HCl using an automated titrator (Metrohm 716 DMS Titrino, Metrohm AG, Herisau, Switzerland) using the Gran method (detection limit 10^{-5} M, uncertainty at $\geq$0.5 mmol·L^{-1} 1–3% and at <0.5 mmol·L^{-1} 7%). The major anion concentrations (Cl^-, SO_4^{2-}) were measured by ion chromatography (HPLC, Dionex ICS 2000, ThermoFisher, Waltham, MA, USA) with an uncertainty of 2%.

Table 1. The physicochemical parameters of groundwater.

Sample ID	Location	H, m.a.s.l.	Sample Date// Depth (m)	T (°C)	pH (Unit)	Eh (mV)	O_2 (mg·L^{-1})	TDS (mg·L^{-1})	Sr (mg·L^{-1})
K-120	N 65.87238 E 44.13921	6	18 June//40–60	5.3	8.03	151	3.0	410	12.09
K-1	N 65.88087 E 44.12091	22	18 June//40–60	7.1	7.99	155	8.0	446	8.23
M-200	N 65.85261 E 44.23201	11	21 June//40–60	4.8	7.90	−60	2.8	469	1.91
M-84	N 65.86652 E 44.21601	13	20 June//40–60	5.3	7.77	73	3.2	473	0.76
M-10	N 65.86009 E 44.23067	10	19 June//40–60	5.5	7.87	−121	2.1	538	17.10
M-20	N 65.83675 E 44.26264	28	21 June//40–60	4.0	7.89	−103	2.2	562	1.50
M-85	N 65.84367 E 44.23960	10	19 June//40–60	5.6	7.82	8	6.0	646	26.31
M-4	N 65.86776 E 44.20915	11	20 June//40–60	4.2	7.45	66	0.6	656	1.02
M-169	N 65.83541 E 44.25338	19	21 June//40–60	5.0	7.78	−58	3.4	663	6.60
M-48	N 65.84318 E 44.24603	12	22 June//40–60	5.3	7.86	−78	2.8	669	4.62
M-44	N 65.84731 E 44.24515	17	22 June//40–60	5.3	7.67	−6	3.0	705	2.40
M-43	N 65.84137 E 44.24300	9	19 June//40–60	6.5	7.61	−109	0.6	731	32.00
M-165	N 65.86820 E 44.22311	17	20 June//40–60	4.6	7.56	58	2.0	752	1.50
M-172	N 65.84790 E 44.23991	13	22 June//40–60	8.2	7.64	38	5.6	780	2.70
K-4	N 65.89190 E 44.11613	10	17 June//40–60	6.0	7.28	−41	4.5	803	40.11
K-5	N 65.89627 E 44.11808	11	17 June//40–60	5.7	7.06	−116	0.0	857	27.14
K-119	N 65.88612 E 44.10291	12	17 June//40–60	5.0	7.67	−16	3.1	979	39.06

Sample ID	Na^+ (mg·L^{-1})	Ca^{2+}	Mg^{2+}	K^+	Cl^-	SO_4^{2-}	HCO_3^-	Ca^{2+}/Sr	Water Type [a] (-)
K-120	24.0	48.3	16.8	3.61	24.8	16.0	265	4.0	Ca-Mg-HCO_3
K-1	18.9	58.1	20.5	3.73	21.2	26.7	289	7.1	Ca-Mg-HCO_3
M-200	23.1	61.3	21.1	3.49	10.6	7.1	341	32.0	Ca-Mg-HCO_3
M-84	19.8	74.1	15.7	3.60	14.2	15.6	330	98.0	Ca-HCO_3
M-10	27.4	64.5	25.2	3.68	38.9	8.3	353	3.8	Ca-Mg-HCO_3
M-20	49.0	65.3	18.7	3.71	10.6	9.2	404	43.0	Ca-Na-HCO_3
M-85	35.4	61.3	29.6	3.91	17.7	85.1	387	2.4	Ca-Mg-HCO_3
M-4	38.9	107.0	9.1	4.25	15.9	56.5	424	107.0	Ca-HCO_3
M-169	55.9	74.9	25.1	4.16	24.8	6.5	465	11.0	Ca-Na-Mg-HCO_3
M-48	39.8	83.0	29.8	3.78	24.8	15.7	467	18.0	Ca-Mg-HCO_3
M-44	54.5	105.0	11.8	4.22	10.6	4.4	512	44.0	Ca-Na-HCO_3
M-43	80.0	49.3	25.1	4.31	33.6	72.9	433	2.2	Na-Ca-HCO_3
M-165	63.9	111.0	21.3	4.62	37.2	36.0	476	74.0	Ca-Na-HCO_3
M-172	72.4	111.0	7.9	3.90	33.6	44.0	494	41	Ca-Na-HCO_3
K-4	43.7	85.0	33.4	4.13	54.9	52.3	489	2.1	Ca-Mg-HCO_3
K-5	84.0	85.4	21.9	6.41	65.8	108.0	458	3.2	Ca-Na-HCO_3
K-119	170.0	58.9	37.2	11.10	158.0	123.0	382	1.5	Na-Mg-Ca-HCO_3-Cl

[a] Cations and anions with a content higher than 25 mg-eq·% are listed in descending order.

Table 2. The mineral saturation indices (SI) of groundwater.

Sample ID	Dolomite	Calcite	Strontianite	Anhydrite	Gypsum	Celestite
K-120	0.88	0.42	1.87	−2.98	−2.56	−2.57
K-1	0.90	0.43	1.64	−2.70	−2.28	−2.54
M-200	0.91	0.44	0.98	−3.25	−2.84	−3.76
M-84	0.58	0.38	0.45	−2.83	−2.42	−3.81
M-10	0.98	0.44	1.92	−3.19	−2.78	−2.76
M-20	1.03	0.54	0.95	−3.13	−2.72	−3.77
M-85	0.84	0.33	2.02	−2.23	−1.82	−1.59
M-4	−0.03	0.27	0.30	−2.16	−1.75	−3.18
M-169	1.08	0.53	1.52	−3.26	−2.85	−3.31
M-48	1.33	0.64	1.44	−2.85	−2.44	−3.10
M-444	0.75	0.60	1.02	−3.29	−2.88	−3.92
M-43	0.38	0.09	1.96	−2.40	−1.98	−1.57
M-165	0.79	0.50	0.69	−2.39	−1.98	−3.25
M-172	0.44	0.55	0.99	−2.28	−1.87	−2.88
K-4	0.16	0.04	1.77	−2.34	−1.93	−1.66
K-5	−0.59	−0.24	1.32	−2.02	−1.61	−1.51
K-119	0.79	0.25	2.14	−2.19	−1.77	−1.35

Table 3. Characteristics of the isotopic composition of groundwater and parameters used to estimate the residence time of groundwater in the aquifer.

Sample ID	^{14}C (pmc)	$\delta^{13}C$ (‰)	^{14}C [a] (pMC)	$^{14}C_0$ [b] (pmc)	$^{14}C_0$ [c]	$^{14}C_0$ [d]	$^{14}C_0$ [e]
K-120	44.04 ± 0.47	−10.6	42.79 ± 0.46	45.00	*NC*	60.42	85
K-1	45.4 ± 0.41	−10.7	44.1 ± 0.4	45.36	*NC*	60.99	85
M-200	50.15 ± 0.53	−9.1	48.56 ± 0.51	39.64	*NC*	51.87	85
M-84	65.02 ± 0.58	−13.2	63.49 ± 0.57	54.29	50.47	76.95	85
M-10	57.45 ± 0.66	−8.7	55.58 ± 0.64	38.21	*NC*	49.59	85
M-20	54.57 ± 0.54	−13.3	53.29 ± 0.53	54.64	53.98	75.81	85
M-85	49.32 ± 0.61	−11.8	49.02 ± 0.59	49.29	*NC*	67.26	85
M-4	74.47 ± 0.66	−14.6	72.92 ± 0.65	59.29	63.17	83.22	85
M-169	60.53 ± 0.65	−15.7	59.4 ± 0.64	63.21	90.87	89.49	85
M-48	58.3 ± 0.54	−15.8	57.23 ± 0.5	63.57	93.62	90.06	85
M-44	61.39 ± 0.60	−13.5	59.98 ± 0.59	55.36	52.79	76.95	85
M-43	44.64 ± 0.55	−9.9	43.29 ± 0.53	42.50	*NC*	56.43	85
M-165	72.2 ± 0.67	−12.0	70.32 ± 0.65	50.00	24.61	68.4	85
M-172	62.87 ± 0.56	−15.2	61.64 ± 0.55	61.43	77.44	86.64	85
K-4	50.24 ± 0.44	−9.8	48.71 ± 0.43	42.14	*NC*	55.86	85
K-5	59.23 ± 0.54	−13.3	57.84 ± 0.53	54.64	21.96	75.81	85
K-119	29.53 ± 0.49	−8.6	28.56 ± 0.47	37.86	*NC*	49.02	85

Sample ID	^{14}C Age [b] (year BP)	^{14}C Age [c]	^{14}C Age [d]	^{14}C Age [e]	U (ppb)	$^{234}U/^{238}U$ (unit)
K-120	424 ± 104	*NC*	2675 ± 163	6171 ± 144	0.130	1.12
K-1	214 ± 213	*NC*	2529 ± 169	5968 ± 204	0.075	1.13
M-200	modern	*NC*	236 ± 235	5027 ± 187	0.243	2.78
M-84	modern	modern	1337 ± 187	2237 ± 82	0.649	1.67
M-10	modern	*NC*	modern	3472 ± 102	0.026	1.63
M-20	208 ± 207	modern	2836 ± 84	4014 ± 128	0.094	1.65
M-85	modern	*NC*	2628 ± 138	5143 ± 163	0.225	2.08
M-4	modern	modern	842 ± 78	1049 ± 121	0.607	1.81
M-169	570 ± 76	3588 ± 109	3468 ± 91	2898 ± 109	0.027	3.48
M-48	804 ± 99	4369 ± 131	4540 ± 240	3336 ± 106	0.108	3.43
M-44	modern	modern	1801 ± 92	2810 ± 65	1.633	1.54
M-43	modern	*NC*	1820 ± 84	6130 ± 136	0.042	2.06
M-165	modern	modern	modern	1259 ± 76	0.994	1.23
M-172	modern	1632 ± 83	2791 ± 61	2605 ± 118	1.885	1.57
K-4	modern	*NC*	817 ± 88	4935 ± 92	0.078	2.26
K-5	modern	modern	2007 ± 104	3186 ± 140	0.085	1.59
K-119	2424 ± 272	*NC*	4662 ± 206	9828 ± 285	0.014	3.94

[a] normalized radiocarbon concentration; [b] initial carbon isotopic composition and calibrated age according to the Pearson model; [c] same for Mook model; [d] same for Ferronsky model; [e] same for Vogel model; *NC* not calculated.

Estimates of the residence time of groundwater in the aquifer were made using carbon isotopes ^{14}C and ^{13}C [40,41]. Two models were used to determine the initial radiocarbon content in the groundwater recharge area ($^{14}C_0$). For isotopic exchange between solid carbonate and total dissolved inorganic carbon (TDIC), the Ingerson and Pearson model was used [42]. For isotope exchange between soil CO_2 and TDIC, the Mook model [43,44] was used (see [38,45]).

Due to the fact that calculations using these models showed a very young age of groundwater, Ferronsky and Polyakov's [46] model to account only for the dissolution of carbonates was also used:

$$^{14}C_0 = -5.7\delta^{13}C \quad (1)$$

In addition, according to Vogel's [47] generalization that the radiocarbon activity of freshly formed groundwater in many parts of the world averages 85 ± 5% of the radiocarbon activity of a modern wood standard, the simplest model was also used:

$$^{14}C_0 = 85pmc \quad (2)$$

Calib Rev 8.1.0 was used to calibrate the radiocarbon ages [48,49].

4. Results

4.1. The Physicochemical Parameters of Groundwater

Physicochemical parameters characterizing the water composition of the Upper Permian Kazan carbonate aquifer (P_2kz) are shown in Table 1 and Section S2 of the Supplementary Materials and illustrated by Piper diagrams in Figure 3.

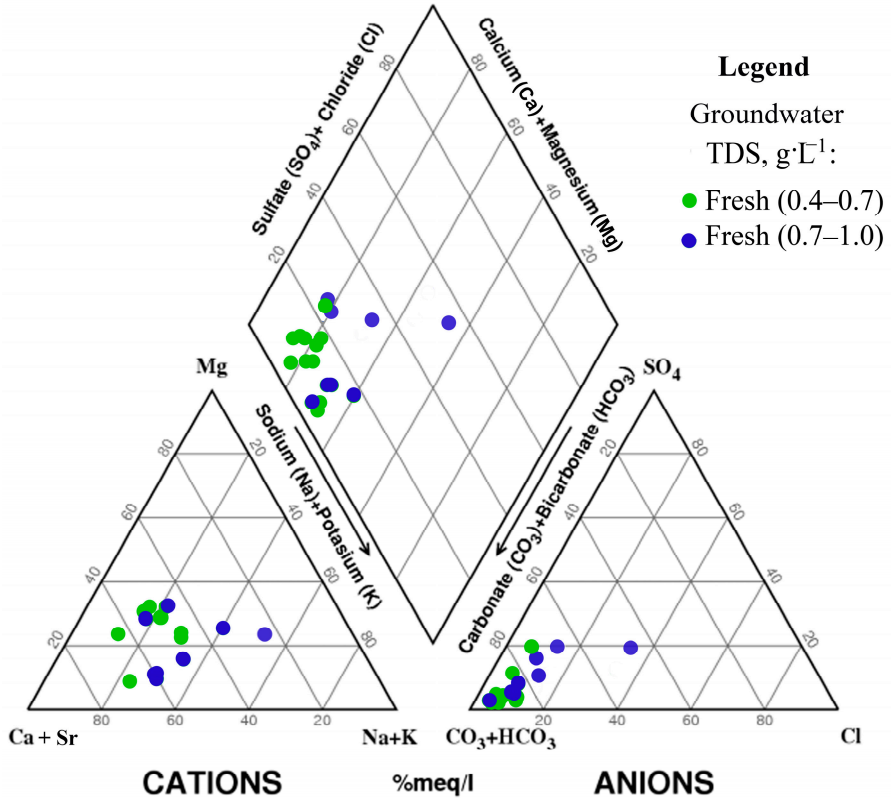

Figure 3. Piper diagrams.

TDS in fresh water ranged from 410 to 979 mg·L^{-1}. The Ca-Mg-HCO_3 composition was typical for low-mineralized waters. With an increase in their mineralization, the chemical composition changed to Ca-Na-HCO_3 and Na-Mg-Ca-HCO_3-Cl. As the composition of the groundwater changed, its pH also changed from the range of 7.45–8.03 (average value = 7.84) to the range of 7.06–7.67 (average value = 7.47). Sr concentrations ranged from 0.76 to 40.11 mg·L^{-1}, regardless of the overall water composition (Table 1). The water saturation indices (SI) for gypsum and anhydrite were largely negative (Table 2), and there was a deficiency of SO_4^{2-} relative to Ca^{2+} (Figure 4a), which indicated relatively small amounts of Ca^{2+} transferred into water due to the dissolution of gypsum. The exception was the most mineralized sample K-119, in which the Ca^{2+}:SO_4^{2-} ratio was close to unity (1.15).

In low-mineralized waters, the ratio (Ca^{2+} + Mg^{2+}):HCO_3^- is close to unity. As the degree of water mineralization increases, a deficiency (Ca^{2+} + Mg^{2+}) is observed (Figure 4b). At the same time, the ratios Na^+:HCO_3^- (Figure 4c) and Na^+:Ca^{2+} (Figure 4d) increase. Sea coasts are characterized by an observed increase in the concentration of chlorine in groundwater up to 158 mg·L^{-1} (see Figures 1a and 2). However, an excess of sodium compared to chlorine (Figure 4f) and negative values of chlor-alkali indices (Figure 4e) indicate the possibility of Na^+ passing into solution due to the cation exchange of alkaline earth elements for alkaline ones [50,51]. Additional sources of sodium can be aluminosilicates such as albite and oligoclase.

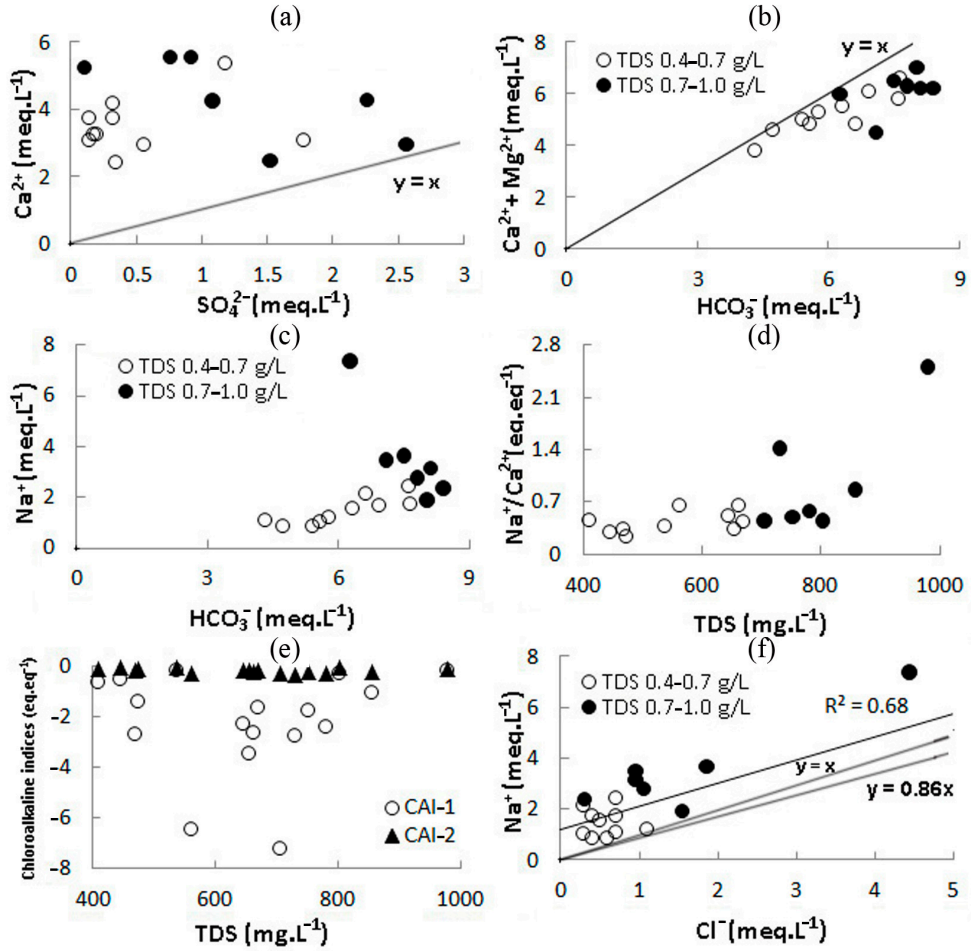

Figure 4. Diagrams showing element concentrations (meq·L^{-1}) and their ratios (eq·eq^{-1}) in the fresh groundwater of the study area with TDS groups; Ca^{2+} vs. SO_4^{2-} (**a**), (Ca^{2+} + Mg^{2+}) vs. HCO_3^- (**b**), Na^+ vs. HCO_3^- (**c**), Na^+/Ca^{2+} vs. TDS (**d**), Chloroalkaline indices vs. TDS (**e**) and Na^+ vs. Cl^- (**f**).

4.2. Isotopic Parameters of Groundwater

The results of determinations of carbon and uranium isotopes in groundwater of the Upper Permian Kazan carbonate aquifer (P_2kz) are presented in Table 3.

As can be seen from the table, the Pearson and Mook models generally provide values for the residence time of groundwater in the aquifer that can be characterized as "modern." Four samples showed values ranging from 1632 ± 83 to 4540 ± 240 years. Calculations using the Ferronsky model showed groundwater age values comparable to those determined by the Mook model approximately up to 4662 ± 206 years, and according to the Vogel model they were twice as high.

In general, for all models, one can see a tendency to correlate the age of groundwater with radiocarbon concentrations in groundwater (Figure S2), and we considered it more logical to use the ^{14}C (pmc) values when analyzing changes in the strontium concentration depending on water age (see Section 4.5).

The ^{14}C values varied from 74.47 ± 0.66 to 29.53 ± 0.49 pmc. They did not correlate with TDS. A more detailed description is given in Section 4.5.

Uranium concentrations were maximum (0.2–1.9 μg·L^{-1}) under oxidizing conditions, where uranium was in the 6^+ form; under reducing conditions, uranium passed into the 4^+ state, and its content, as a rule, does not exceed 0.1 μg·L^{-1} (Figure S3a). The maximum concentrations of uranium tended to be in more alkaline conditions than the minimum concentrations (pH 7.5–8; Figure S3b), where they were in the composition of uranyl-carbonate complexes. The maximum concentrations of uranium also predominated in younger waters (^{14}C = 60–80 pmc) when compared to the minimal concentrations

(^{14}C = 20–60 pmc; Figure S3c). In waters with maximum uranium concentrations, where rock dissolution processes predominate, the ratio of uranium isotopes ^{234}U:^{238}U was minimal (1–2); in reducing conditions where recoil loss factors predominate, it rose to 4 (Figure S3d). Under oxidizing conditions, elevated uranium concentrations correlated with TDS (R^2 = 0.59; Figure S3e) and the main TDS-determining ions—Na^+ (R^2 = 0.73; Figure S3f), HCO_3^- (R^2 = 0.75; Figure S4a), and Ca^{2+} (R^2 = 0.67; Figure S4b)—but did not correlate with SO_4^{2-}, Cl^-, or Mg^{2+} (Figure S4c–e). Under reducing conditions, there was no correlation between the minimum concentrations of uranium, TDS, and basic ions.

4.3. Dependence of Strontium on the Acid–Base and Redox Properties of Fresh Water in the Upper Permian Kazan Carbonate Aquifer (P_2kz)

Elevated strontium concentrations showed a tendency to increase simultaneously with a decrease in pH to neutral values (Figure 5a), although the significance level for this dependency was above 5% (coefficient of determination R^2 = 0.44, coefficient of correlation r = –0.67, significance value p = 0.07; see Section S3 of the Supplementary Materials). For low strontium concentrations there was no correlation (R^2 = 0.09, r = 0.31, p = 0.42).

The dependence of the SI values for calcite and dolomite on pH was well pronounced for groundwater with high strontium concentrations (R^2 = 0.93–0.88, r = 0.97–0.94, p = 0). At the same time, the supersaturation of water in relation to these minerals was replaced by undersaturation, which was characterized by a change in SI from 0.4 and 1 to –0.2 and –0.6, respectively, as it approached neutral pH values (Figure 5b). There was practically no tendency to increase Sr in this direction (Figure 5g) (R^2 = 0.35 and 0.18, r = –0.59 and –0.43, p = 0.12 and 0.29, respectively).

A correlation between saturation indices for dolomite and pH was observed in groundwater with low strontium concentrations (R^2 = 0.64, r = 0.8, p = 0.01), with SI changing from 1.3 to –0.03. There was no correlation between SI values for calcite and pH (R^2 = 0.19, r = 0.45, p = 0.22), with SI changing from 0.6 to 0.3. The concentration of Sr increased in the direction of increasing the supersaturation of water with respect to calcite and dolomite (R^2 = 0.30–0.34, r = 0.56–0.58, p = 0.12–0.1), which may indicate other sources of Sr in the water.

The SI values for strontianite did not correlate with pH (R^2 = 0.28 and 0.34, r = 0.53 and 0.58, p = 0.18 and 0.1 for water samples with high and low strontium concentrations, respectively; Figure 5c). The same can be said about the concentration of Sr in water with a high content of it. Low strontium concentrations increased towards increasing the water supersaturation with strontianite from SI 0.3 to 1.5 (Figure 5h) (R^2 = 0.79, r = 0.89, p = 0.01).

Negative saturation indices for gypsum and celestite were recorded throughout the entire range of their values. For water with high strontium contents they increased as they approached neutral pH values from –2.8 to –1.6 and –1.4, respectively (Figure 5b,c) (R^2 = 0.49–0.45, r = –0.7 to –0.67, p = 0.05 –0.07). The concentrations of strontium increased in a similar manner (Figure 5g,h) (R^2 = 0.48–0.74, r = 0.7–0.86, p = 0.06–0.006). For samples with low strontium contents, SI increased from −2.9 and −3.9 to −1.8 and −2.9, respectively (Figure 5b,c) (R^2 = 0.59–0.18, r = –0.76 to –0.42, p = 0.02–0.26); however, they were not correlated with Sr (Figure 5g,h) (R^2 = 0.14–0.12, r = –0.37 to 0.35, p = 0.32–0.36).

There was a dependence of TDS on pH (R^2 = 0.56, r = –0.75, p = 0.03 in water samples with high strontium contents and R^2 = 0.36, r = –0.6, p = 0.09 in water samples with low strontium contents), which was expressed with an increase in TDS as the pH approached neutral values in the P_2kz carbonate aquifer (Table 1). Elevated strontium concentrations showed a high positive correlation with TDS (Figure 5d) (R^2 = 0.82; r = 0.9, p = 0.002). Low strontium concentrations did not correlate with TDS (R^2 = 0.09, r = 0.3, p = 0.43).

As in the case of pH, for groundwater with a high content of strontium, a slight decrease in the supersaturation of water in calcite and dolomite was found as the degree of water mineralization increased (R^2 = 0.49–0.31; Figure 5e). Saturation indices for strontianite did not correlate with TDS (R^2 = 0.01; Figure 5f). The most pronounced undersaturation of water was with respect to gypsum and celestite (Figure 5e,f), and this undersaturation

decreased as TDS increased from SI = –2.8 to –1.6 and from –2.8 to –1.4, respectively (R^2 = 0.64–0.73, r = 0.8 –0.89, p = 0.02–0.003). For groundwater with a low content of strontium, there was no correlation of TDS with saturation indices for all minerals except celestite (Figure 5e,f).

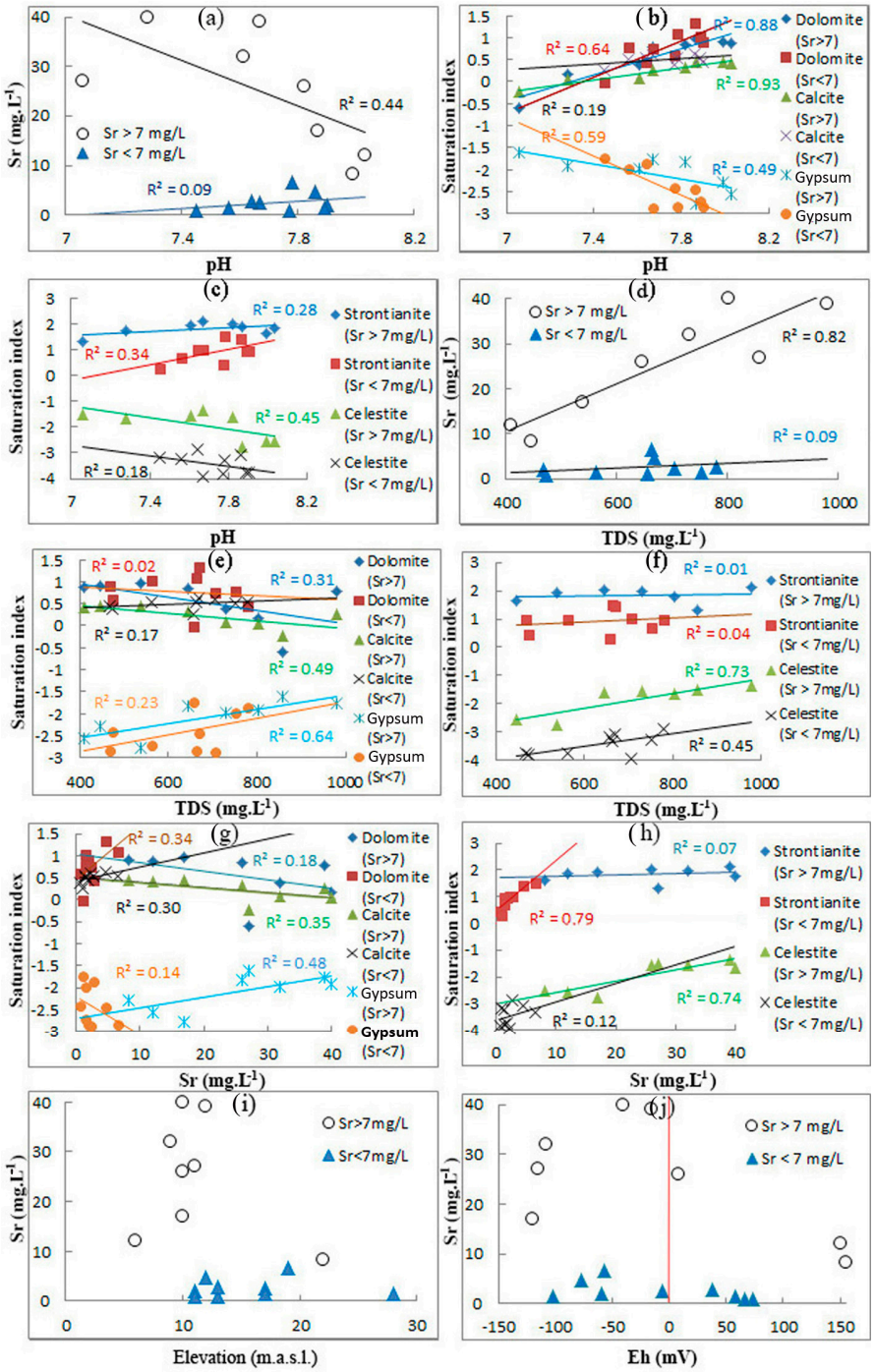

Figure 5. Graphs of strontium concentrations in water as a function of pH (**a**), TDS (**d**), SI (**g**,**h**), elevation (**i**), and Eh (**j**); graphs of groundwater saturation indices depending on pH (**b**,**c**) and TDS (**e**,**f**). Red line is Eh = 0.

Groundwater with high Sr concentrations tended to predominate in the lowlands near the river (Figure 5i) and in the reducing conditions of the aquifer (Figure 5j). Figure 6a shows the correlation between the maximum Sr concentrations and the minimum U concentrations characteristic of a reducing environment in aquifers [52] (see Table 2). Figure 6b

also demonstrates the presence of two different correlation trends for the maximum and minimum Sr concentrations with ^{234}U:^{238}U activity ratios, with the same correlation coefficients (R^2 = 0.64). A similar trend (without separation of water types according to Sr concentrations) was noted by Plechacek et al. [30].

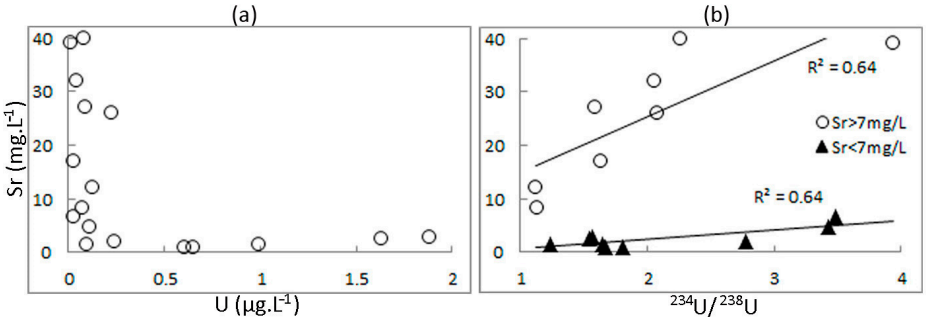

Figure 6. Graphs of strontium concentrations in water as a function of U (**a**) and $^{234}U/^{238}U$ (**b**) in the fresh groundwater.

4.4. Strontium vs. Chemical Composition of the Fresh Groundwater in the Upper Permian Kazan Carbonate Aquifer

Figures 5d and 7a,b show that increased strontium concentrations were correlated with TDS, Mg^{2+}, and HCO_3^- (R^2 = 0.82–0.69, r = 0.91–0.83, p = 0.002–0.01). There was a trend of increasing Sr concentrations with increasing SO_4^{2-}, Na^+, and Cl^- (Figure 7c–e) (R^2 = 0.5–0.38, r = 0.71–0.62, p = 0.05–0,1). There was virtually no correlation with Ca^{2+} (R^2 = 0.16; Figure 7f).

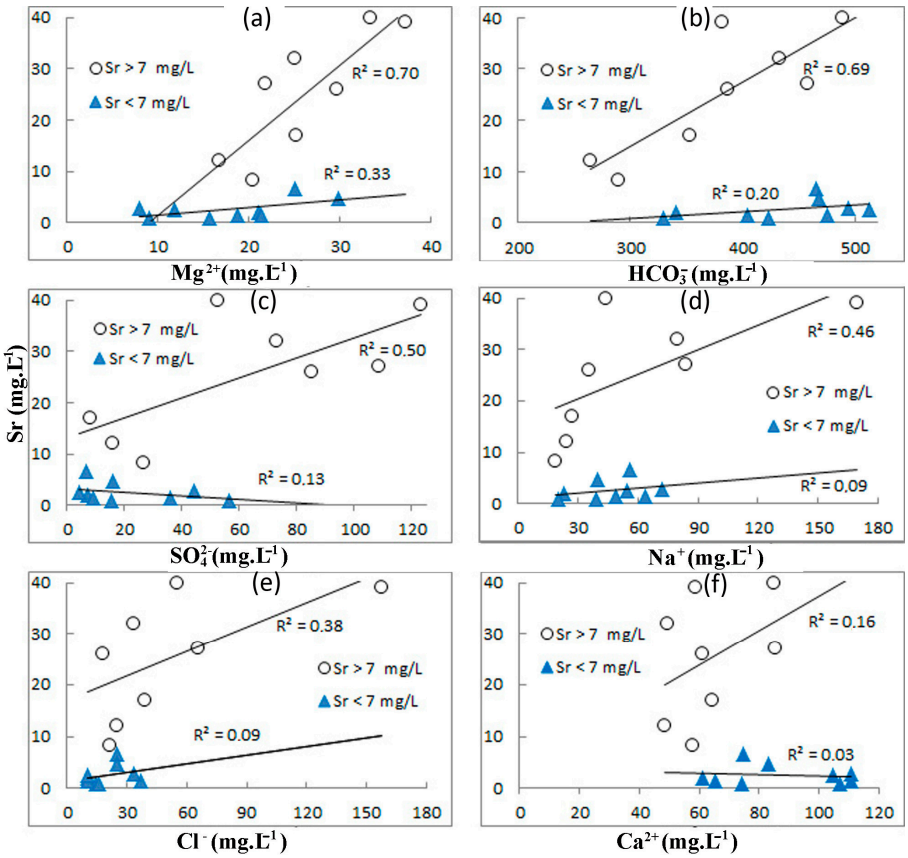

Figure 7. Graphs of strontium concentrations in water as a function of Mg^{2+} (**a**), HCO_3^- (**b**), SO_4^{2-} (**c**), Na^+ (**d**), Cl^- (**e**), and Ca^{2+} (**f**).

For these waters, a close dependence of the contents of sulfates and sodium on the total amount of dissolved substances was also recorded (R^2 = 0.77–0.72) (Figure 8a). The dependence of TDS on the contents of chlorides, bicarbonates, and magnesium was somewhat lower (R^2 = 0.62–0.52), and the correlation with calcium was practically absent (R^2 = 0.23).

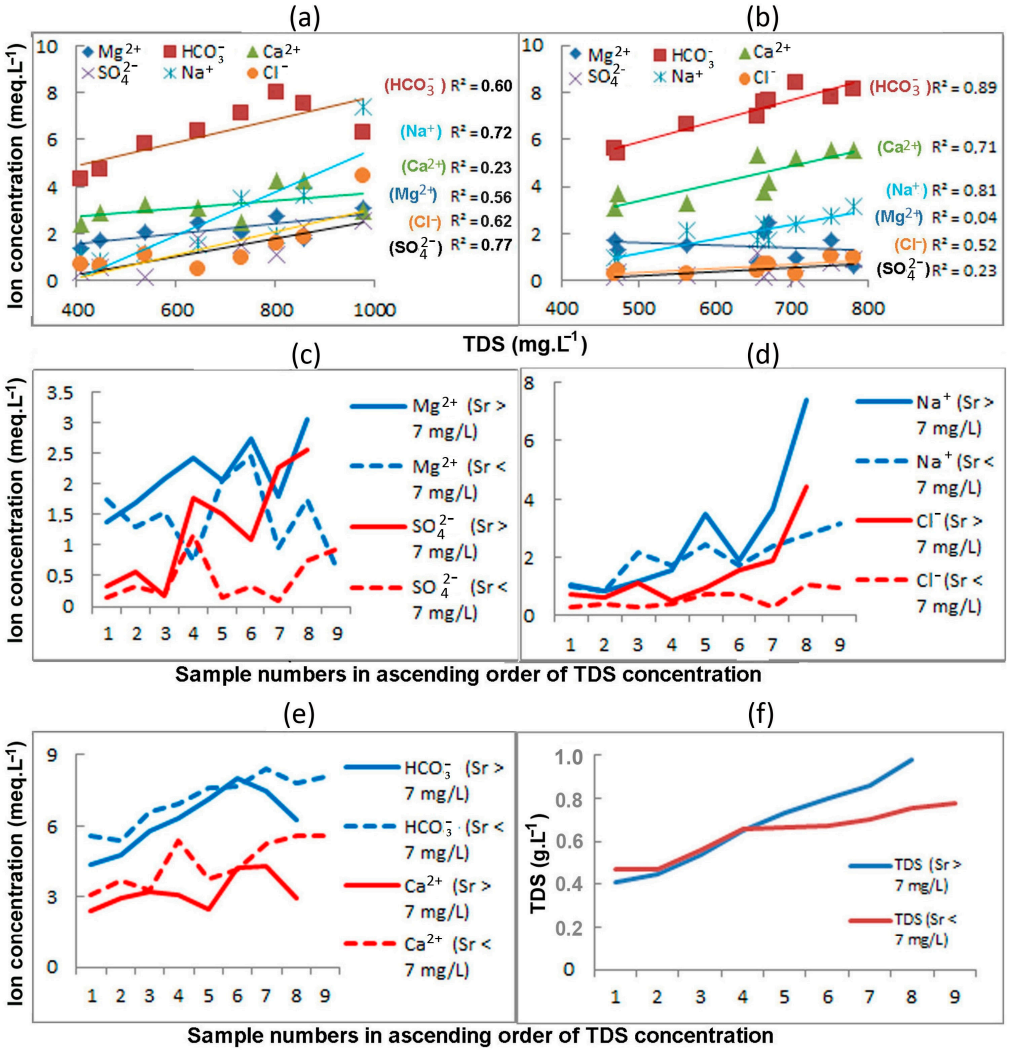

Figure 8. Diagrams of the dependence of the contents of the main cations and anions on the total amount of dissolved substances in water with excesses of the PMC for strontium (**a**) and in water of standard quality (**b**); the ratio of the concentrations of main cations and anions in waters of these two types (**c**–**f**).

Figure 8c,d show that the contents of Mg^{2+}, SO_4^{2-}, Na^+, and Cl^- in water with strontium concentrations above the MPS are noticeably higher than in water of standard quality; the concentrations of HCO_3^- and Ca^{2+} show the opposite pattern (Figure 8e).

In addition, in water of standard quality there was no correlation between strontium contents and the ionic composition and total amount of dissolved substances (Figures 5d and 7). At the same time, there was a close dependence of TDS on the contents of bicarbonates, sodium, and calcium (R^2 = 0.89–0.71; Figure 8b). It was somewhat lower in relation to chlorides (R^2 = 0.52) and was practically absent in relation to sulfates and magnesium (R^2 = 0.23 and 0.04).

4.5. Dependence of Strontium Content on Water Age

Figure 9a shows a decrease in Ca^{2+} concentrations with decreasing ^{14}C (pmc) values, that is, increasing age of water. At the same time, the concentrations of Sr and Mg^{2+} increased, and in Figure 9c,d a clear increase in Mg^{2+}:Ca^{2+} and Sr:Ca^{2+} can be seen. It should be noted that these graphs were built for the entire data set (17 water samples). For water with high (8 samples) and low (9 samples) Sr content, a weak correlation was found between ^{14}C and Ca^{2+} (Figure 9b) (R^2 = 0.30–0.58, r = 0.55–0.76, p = 0.16–0.02); there is no correlation between ^{14}C and Sr (R^2 = 0.07–0.08, r = –0.27 to –0.28, p = 0.52 to 0.46).

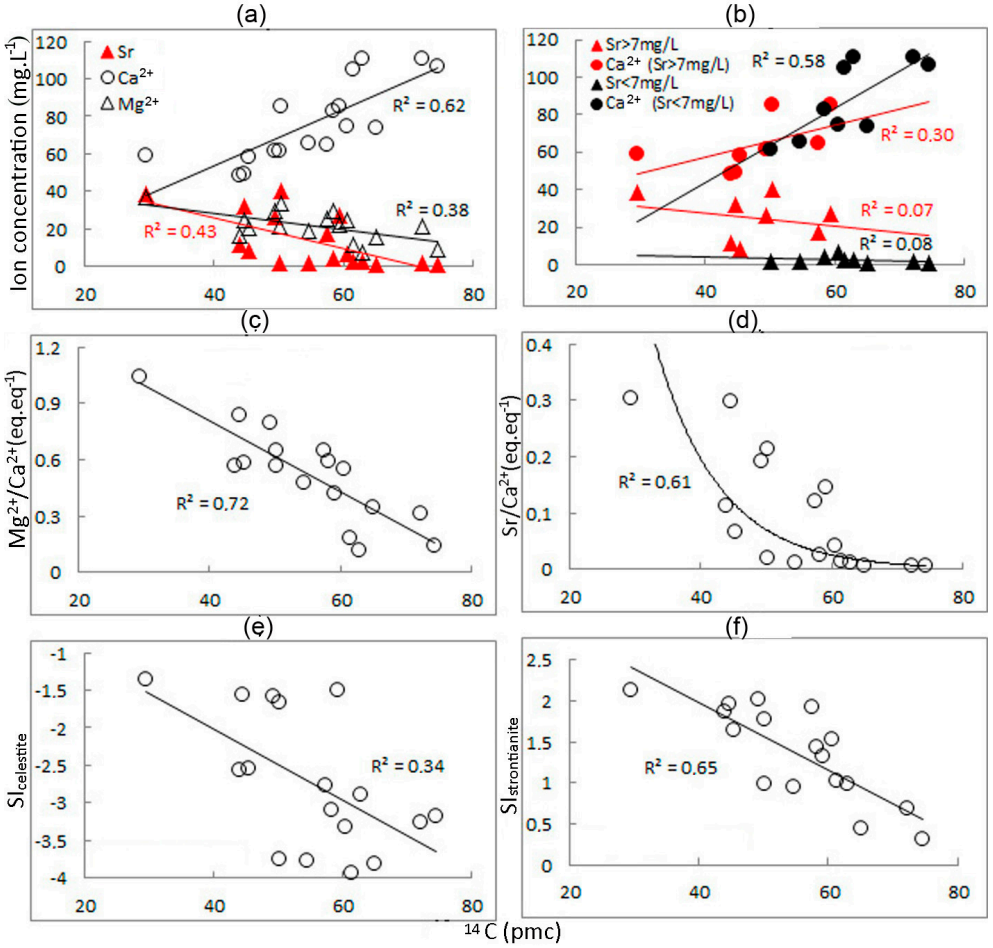

Figure 9. ^{14}C (pmc) vs. (**a**) strontium, calcium, and magnesium; (**b**) strontium and strontium in high and low-Sr water; (**c**) Mg^{2+}:Ca^{2+}; (**d**) Sr:Ca^{2+}; (**e**) $SI_{celestite}$; (**f**) $SI_{strontionite}$.

Graphs constructed from the entire data set (17 water samples) (Figure 9e,f) also show a correlation of SI for strontianite with the age of water (R^2 = 0.65) and a weak correlation of SI for celestite with the age of water (R^2 = 0.34). In water of standard quality (9 samples), there was also a correlation of SI for strontianite with the age of water (r = –0.61, p = 0.047) and no correlation of SI for celestite with the age of water (r = 0.41, p = 0.27). In water exceeding the MPC for strontium, the correlation of the saturation indices of strontianite and celestite with the age of the water was not established (r = –0.64 and –0.27, p = 0.08 and 0.52).

5. Discussion

5.1. Groundwater with Strontium Concentrations above the MPC

We have shown above that an increase in strontium concentrations in fresh groundwater was observed simultaneously with an increase in the amount of dissolved substances and a decrease in pH to approximately neutral values. Similar trends were also noted by

Krainov [2] and Macgrove [29]. However, the correlation of strontium and pH in our case was insignificant (r = –0.67, p = 0.07) compared to the correlation of strontium and the amount of dissolved substances (r = 0.9, p = 0.002). As a result, there was a clear increase in the values of $SI_{celestite}$ and SI_{gypsum} simultaneously with an increase in the content of dissolved substances in water (r = 0.89–0.8, p = 0.003–0.02), while the correlation of $SI_{celestite}$ and SI_{gypsum} with pH was noticeably less pronounced (r = –0.67 and –0.7, p = 0.07 and 0.05). There was also a clear increase in strontium concentration along with an increase in $SI_{celestite}$ and SI_{gypsum} (r = 0.86–0.7, p = 0.006–0.06), while water saturation with calcite and dolomite had little effect on the increase in strontium content. A relationship between $SI_{celestite}$ and $SI_{strontianite}$ and the age of groundwater was noted.

A correlation of magnesium with strontium and total mineralization of groundwater (r = 0.84 and 0.75, p = 0.01 and 0.03) and no correlation of calcium with strontium and total mineralization of groundwater (r = 0.4 and 0. 48, p = 0.32 and 0.23) were found for strontium-rich groundwater. In addition, it was found that with increasing water age, there was a decrease in calcium concentration with a parallel increase in strontium and magnesium concentrations and an increase in magnesium–calcium and strontium–calcium ratios.

Thus, it can be assumed that it is not an increase in magnesium concentrations as a result of the dedolomitization of rocks [23,29,53–55], but a decrease in the calcium concentrations (Figures 9a and 10) that causes an increase in the content of strontium, which replaces it.

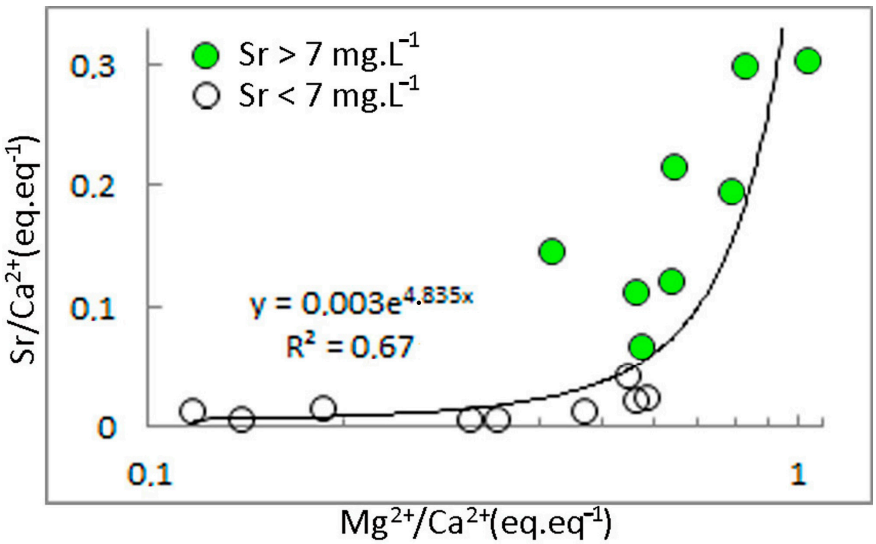

Figure 10. $Sr:Ca^{2+}$ vs. $Mg^{2+}:Ca^{2+}$ plot.

However, a separate analysis of age-related changes in the concentrations of Ca and Sr in waters with strontium contents above and below the MPC (Figure 9b) shows less certain dependencies, and therefore it is advisable to check them in the future using more extensive material through periodical samplings.

The correlation of strontium with bicarbonate ions is also significant (r = 0.83, p = 0.01), since bicarbonate ions are one of the main components of low-mineralized water. However, in more mineralized waters they are partially "replaced" by sulfate ions and chloride [24,25] (see Figure 8a,c–e). At the same time, as shown above, calcium concentrations increased in proportion to the concentrations of bicarbonate ions, also in low-mineralized waters, and then were partially "replaced" by sodium (see Figure 8e,d).

Based on the established correlation of the concentrations of strontium (Figure 5d), chlorine ions, and sodium (Figure 8d) with the total mineralization of groundwater and the tendency of increasing strontium concentrations with increasing sodium and chlorine content, it can be assumed that there is an influence of the upwelling of salt waters from the lower substage of the Kazan aquifer (see Figure 2) to increase the strontium content in

drinking water. According to [26], the contents of TDS and Sr in saline groundwater are 3100 and 9 ppm, respectively. That is, water mineralization up to 700–1000 ppm can be obtained by mixing one part of salt water with 4–8 parts of fresh water (400 ppm). However, to achieve a Sr concentration in this mixture of 7 ppm, its concentration in fresh water should already be about 6.6 ppm: (9 x 1 + 6.6 x 6)/7 = 7. That is, the effect of salt water is insignificant in relation to the increase in strontium concentration [56].

The correlation of strontium with sulfate ions and a significant increase in the concentration of sulfate ions with an increase in TDS, as well as the correlation of strontium with $SI_{celestite}$ and SI_{gypsum} indicate the formation of high concentrations of strontium due to the dissolution of these minerals.

The occurrence of the collected water samples with a high content of strontium in the zone of reducing conditions is possibly due to the difficult water exchange in this area and its relatively weak flushing, as a result of which celestite inclusions are preserved there. Other researchers have noted a similar trend [29,30].

The regularity of this factor is also justified by the increase in strontium concentrations in boreholes gravitating to the lowlands near the river (see Figure 1c, Kamenka village and Figure 11).

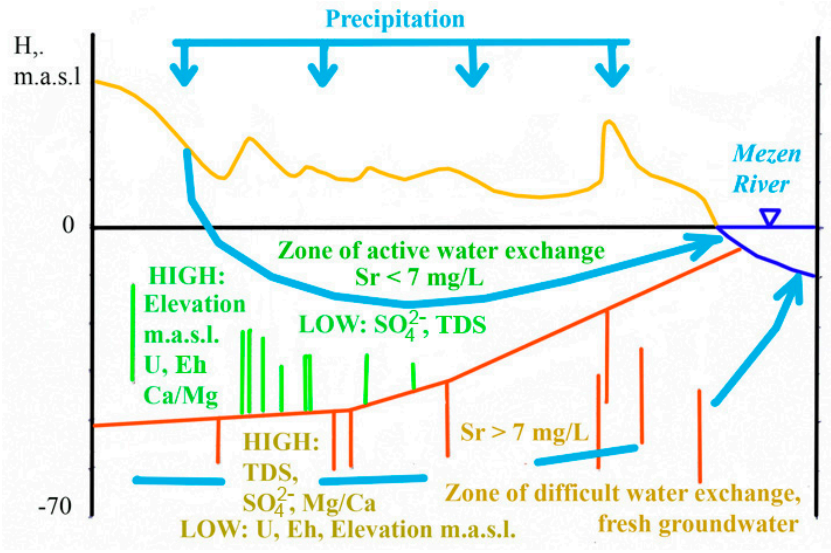

Figure 11. Scheme of the formation of strontium contamination. Green and red vertical lines are groundwater sampling intervals.

5.2. Groundwater with Strontium Content below the MPC

Strontium concentrations in strontium-poor groundwater did not correlate with pH or TDS. Their average values fluctuated around 2.6 $mg \cdot L^{-1}$. Water with strontium content below the MPC was characterized by reduced saturation in relation to $SrSO_4$ and $CaSO_4$, and strontium did not correlate with $SI_{celestite}$ and SI_{gypsum}. Water was supersaturated in $CaCO_3$, $CaMg(CO_3)_2$, and $SrCO_3$; as its supersaturation decreased, the strontium content in water also decreased.

Strontium concentrations in strontium-poor groundwater also did not correlate with major groundwater ions. The concentrations of most ions were noticeably lower than in groundwater with a high content of strontium. The exceptions are bicarbonate ions and calcium. The SO_4^{2-} content was most significantly reduced (Figure 8c), and there was no dependence of strontium concentrations on sulfate ($r = -0.36$, $p = 0.34$), which indicates the formation of strontium due to leaching of discretely distributed small inclusions of $SrSO_4$ and $CaSO_4$. Chloride and sodium concentrations were also reduced, indicating less upwelling of the salty groundwater. But assessments of its influence showed that the upwelling effect of brackish waters on increasing strontium concentrations is significant

(44%) [56]. The dedolomitization processes had virtually no effect on Sr concentrations (Figure 10).

Thus, the main factors characteristic of groundwater with strontium content above the MPC (correlation of Sr with TDS and $SI_{celestite}$ and SI_{gypsum} and the effect of dedolomitization) were not manifested in groundwater with strontium content below the MPC.

5.3. Estimation of Exposure and Human Health Risk

Data on the carcinogenicity of strontium are very limited, and there is insufficient information to assess its carcinogenic potential due to the lack of adequate studies on long-term chronic exposure [57].

The assessment of non-carcinogenic risk to human health from contact with groundwater was carried out in accordance with the procedure described by the US Environmental Protection Agency [33,57,58]. A deterministic approach was used for two routes of exposure (ingestion and water through the skin) to two subpopulations (adults and children). It is important to emphasize that strontium is not volatile, thus inhalation exposure is not likely, and therefore inhalation was not included in the risk assessment models in this study.

The methodology for assessing exposure and risk to human health, as well as the main parameters and values used for deterministic exposure calculations, are provided in Section S4 Supplementary Materials.

The calculation results are shown in Figure 12:

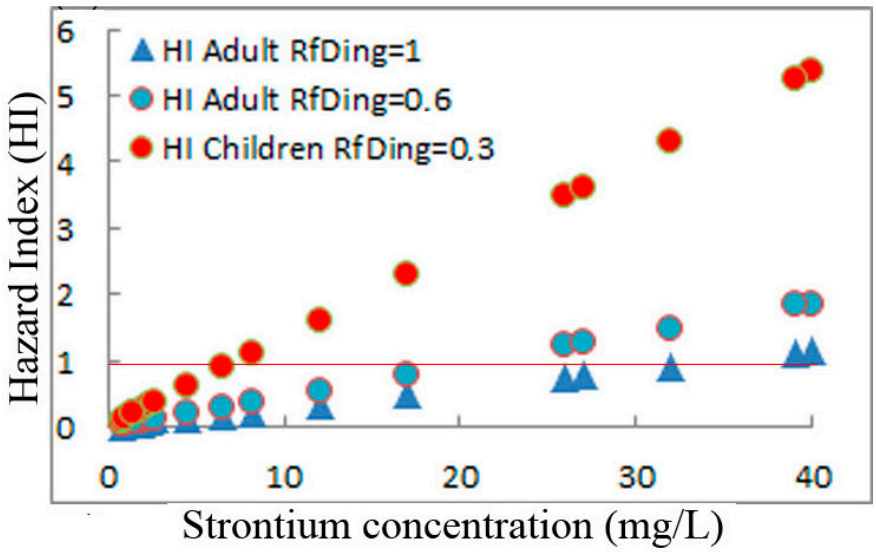

Figure 12. Hazard index (HI) to assess the overall non-carcinogenic health risk from combined ingestion and skin exposure of investigated fresh drinking waters.

Values of HI lower than one indicate no significant non-cancer health risk. Values of HI greater than one depict an existing likelihood of non-cancer health effects occurring and the probability increases as the values rise (see Section S4 Supplementary Materials).

Children in the area are most vulnerable to risks. Fifty percent of the wells contain water that is dangerous for consumption by children of about nine years of age weighing 30 kg. For younger children, the situation is even worse.

For adults weighing up to 70 kg, water from about a third of the studied wells is dangerous.

6. Conclusions

The purpose of this research was to determine natural factors that contribute to maintaining the standard quality of fresh drinking groundwater in areas with high strontium content. The results showed that:

(1) For waters with strontium concentrations above the MPC, the following features are characteristic:
   - Correlations of strontium with TDS and saturation indices for celestite and gypsum, indicating the formation of these waters in sediments with high contents of celestite and gypsum.
   - An increase in strontium–calcium and magnesium–calcium ratios during the period when groundwater is in the aquifer, associated with the process of dedolomitization.
   - Correlation of strontium concentrations with the concentrations of the main ions, except for calcium.
   - Reducing conditions in the aquifer, indicating difficult water exchange in the aquifer, promoting the preservation of strontium-containing minerals.

(2) For waters with strontium concentrations below the MPC, the following features are characteristic:
   - Strontium concentrations do not correlate with TDS, $SI_{celestite}$, and SI_{gypsum}, indicating the formation of water in sediments with discretely located small inclusions of celestite and gypsum.
   - The processes of dedolomitization practically do not affect the growth of strontium concentrations.
   - Oxidizing conditions and active water exchange in the aquifer are favorable for the formation of water with standard quality.

In general, areas of development of groundwater of a Ca-HCO_3 composition with reduced values of the total content of dissolved substances and increased values of the oxidation-reduction potential will be favorable for obtaining drinking water of standard quality.

The assessment of non-carcinogenic risk to human health from contact with groundwater has shown that children in this area are currently the most vulnerable to risks. Fifty percent of wells contain water that is dangerous to drink.

Supplementary Materials: The following supporting information can be downloaded at: https://www.mdpi.com/article/10.3390/w15213846/s1, S1. Statistical distribution of strontium concentration values in drinking groundwater in the North-West of Russia; S2. Summary statistics on compositions of drinking groundwater in the North-West of Russia; S3. Correlation matrices on compositions of drinking groundwater in the North-West of Russia; S4. Estimation of exposure and human health risk; Figure S1. Histograms (a) all 17 samples, (b) 9 samples with strontium contents less than 7 mg/L, (c) 8 samples with strontium contents more than 7 mg/L; Figure S2. Plots of the radiocarbon/residence time in the fresh groundwater Pearson model (a), Ferronsky model (b), and Vogel model (c); Figure S3. Plots of the U concentration in the fresh groundwater vs. Eh (a), pH (b), ^{14}C (c), $^{234}U/^{238}U$ (d), TDS (e), Na^{2+} (f). (Ox)—oxidizing conditions in the aquifer, (Red)—reducing conditions in the aquifer; Figure S4. Plots of the U concentration in the fresh groundwater vs. HCO_3^- (a), Ca^{2+} (b), SO_4^{2-} (c), Cl^- (d), Mg^{2+} (e). (Ox)—oxidizing conditions in the aquifer, (Red)—reducing conditions in the aquifer. Table S1. Summary statistics on strontium concentration values. Table S2. Test of Normality Shapiro-Wilk. Table S3. Parameters and values used for deterministic exposure calculations. Refs [59–64] cited in Supplementary Materials.

Funding: This research was funded by the Russian Science Foundation, grant number 23-27-10004, https://rscf.ru/project/23-27-10004/. (accessed on 10 September 2023).

Data Availability Statement: Data are available upon reasonable request from the corresponding author.

Conflicts of Interest: The author declares no conflict of interest.

References

1. Zektser, I.S. Groundwater as a Component of the Environment. In *Geology and Ecosystems*; Zektser, I.S., Marker, B., Ridgway, J., Rogachevskaya, L., Vartanyan, G., Eds.; Springer: Boston, MA, USA, 2006; pp. 91–105. [CrossRef]
2. Krainov, S.R.; Ryzhenko, B.N.; Shvets, V.M. *Geochemistry of Groundwater. Fundamental, Applied and Environmental Aspects*; CenterLitNefteGaz: Moskow, Russia, 2012; p. 672. (In Russian)

3. Shen, J.; Schäfer, A. Removal of fluoride and uranium by nanofiltration and reverse osmosis: A review. *Chemosphere* **2014**, *117*, 679–691. [CrossRef]
4. Vaiopoulou, E.; Gikasb, P. Regulations for chromium emissions to the aquatic environment in Europe and elsewhere. *Chemosphere* **2020**, *254*, 126876. [CrossRef]
5. He, X.; Li, P.; Shi, H.; Xiao, Y.; Guo, Y.; Zhao, H. Identifying strontium sources of flowback fluid and groundwater pollution using 87Sr/86Sr and geochemical model in Sulige gasfield, China. *Chemosphere* **2022**, *306*, 135594. [CrossRef] [PubMed]
6. *SanRaR 2.1.4.1074-01*; Drinking Water. Hygienic Requirements for Water Quality of Centralized Drinking Water Supply Systems. Quality Control. Sanitary and Epidemiological Rules and Regulations Approved by the Chief State Sanitary Doctor of the Russian Federation on 26 September 2001. Russian Federation: Moscow, Russia, 2001. (In Russian)
7. Amata, R.; Diamond, G.L.; Dorsey, A.; Fransen, M.E. *Toxicological Profile for Strontium*; U.S. Department of Health and Human Services, Public Health Service, Agency for Toxic Substances and Disease Registry: Atlanta, GA, USA, 2004.
8. Bartley, J.C.; Reber, E.F. Toxic effects of stable strontium in young pigs. *J. Nutr.* **1961**, *75*, 21–28. [CrossRef] [PubMed]
9. Colvin, L.B.; Creger, C.R. Stable strontium and experimental bone anomalies. *Fed. Proc. Fed. Am. Soc. Exp. Biol.* **1967**, *26*, 416.
10. Colvin, L.B.; Creger, C.R.; Ferguson, T.M.; Crookshank, H.R. Experimental epiphyseal cartilage anomalies by dietary strontium. *Poult. Sci.* **1972**, *51*, 576–581. [CrossRef] [PubMed]
11. Keesari, T.; Sabarathinam, C.; Sinha, U.K.; Pethaperumal; Thilagavathi, R.; Kamaraj, P. Fate and transport of strontium in groundwater from a layered sedimentary aquifer system. *Chemosphere* **2022**, *307*, 136015. [CrossRef] [PubMed]
12. Khandare, A.L.; Validandi, V.; Rajendran, A.; Singh, T.G.; Thingnganing, L.; Kurella, S.; Nagaraju, R.; Dheeravath, S.; Vaddi, N.; Kommu, S.; et al. Health risk assessment of heavy metals and strontium in groundwater used for drinking and cooking in 58 villages of Prakasam district, Andhra Pradesh, India. *Env. Geochem. Health* **2020**, *42*, 3675–3701. [CrossRef]
13. Zamana, L.V.; Rikhvanov, L.P.; Soktoev, B.R.; Baranovskaya, N.V.; Epova, E.S.; Solodukhina, M.A.; Mikhailova, L.A.; Kopylova, Y.G.; Khvashchevskaya, A.A. New data on chemical composition of natural waters in the area of distribution of Urov (Kaschin–Beck) disease (Transbaikal region). *Bull. Tomsk Polytech. Univ. Geo Assets Eng.* **2019**, *330*, 121–133. (In Russian)
14. Höllriegl, V.; München, H.Z. Strontium in the environment and possible human health effects. *Encycl. Environl. Health* **2011**, *10*, 268–275. [CrossRef]
15. Wang, Z. A historic overview of research and control on Kashin-Beck Disease in China. *Chin. J. Endem.* **1999**, *18*, 161–163.
16. Levander, O.A. Selenium. In *Trace Elements in Human and Animal Nutrition*; Mertz, W., Ed.; Academic Press Inc.: Orlando, FL, USA, 1986; Volume 2, pp. 209–279.
17. Malaisse, F.; Mathieu, F. (Eds.) *Big Bone Disease, a Multidisciplinary Approach of Kashin–Beck Disease in Tibet Autonomous Region (PR China)*; Les Presses Universitaires de Gembloux: Gembloux, Belgium, 2008; p. 148.
18. Vinogradov, A.P. Geochemical investigations in the area of Urov endemia. *Dokl. Akad. Nauk* **1939**, *23*, 64–67. (In Russian)
19. Ermakov, V.V.; Gulyaeva, U.A.; Tyutikov, S.F.; Kuzmina, T.G.; Safonov, V.A. Biogeochemistry of calcium and strontium in the landscapes of Eastern Transbaikalia. *Geochem. Int.* **2017**, *55*, 1105–1117. [CrossRef]
20. Ermakov, V.; Bech, J.; Gulyaeva, U.; Tyutikov, S.; Safonov, V.; Danilova, V.; Roca, N. Relationship of the mobile forms of calcium and strontium in soils with their accumulation in meadow plants in the area of Kashin–Beck endemia. *Env. Geochem. Health* **2020**, *42*, 159–171. [CrossRef] [PubMed]
21. Rikhvanov, L.P.; Soktoev, B.R.; Baranovskaya, N.V.; Ageeva, E.V.; Belyanovskaya, A.I.; Deriglazova, M.A.; Yusupov, D.V.; Epova, E.S.; Solodukhina, M.A.; Zamana, L.V.; et al. Integrated geochemical studies of the components of the natural environment in the endemic regions of Transbaikalia. *Bull. Tomsk. Polytech. Univ. Geo Assets Eng.* **2021**, *332*, 7–25. (In Russian)
22. Vsevolozhsky, V.A. *Fundamentals of Hydrogeology*; Publishing House of Moscow State University: Moscow, Russia, 2007; p. 448. (In Russian)
23. Bui, D.T.; Khosravi, K.; Karimi, M.; Busico, G.; Khozani, Z.S.; Nguyen, H.; Mastrocicco, M.; Tedesco, D.; Cuoco, E.; Kazakis, N. Enhancing nitrate and strontium concentration prediction in groundwater by using new data mining algorithm. *Sci. Total Environ.* **2020**, *715*, 136836. [CrossRef]
24. Limantseva, O.A.; Ryzhenko, B.N. Model for Sr accumulation in the Carboniferous deposits of the Moscow artesian basin. *Geochem. Int.* **2008**, *46*, 935–944. [CrossRef]
25. Limantseva, O.A.; Ryzhenko, B.N.; Cherkasova, E.V. Model for the formation of fluorine-bearing rocks in the Carboniferous deposits of the Moscow artesian basin. *Geochem. Int.* **2007**, *45*, 900–917. [CrossRef]
26. Ivanova, N.I. Strontium distridution patterns in groundwater and aquifer host rocks in the southeastern part of the Severnaya Dvina artesian basin. *Mosc. Univ. Geol. Bull.* **2014**, *69*, 258–266. [CrossRef]
27. Ivanova, I.S.; Shvartsev, S.L.; Pokrovsky, O.S. Distribution of strontium in groundwater of the upper hydrodynamic zone of the Sredneobsky artesian basin (Tomsk region). In *Geological Evolution of the Interaction of Water with Rocks*; Zamana, L.V., Shvartsev, S.L., Eds.; Publishing House of BSC SB RAS: Ulan-Ude, Russia, 2018; pp. 110–114.
28. Kaleem, M.; Naseem, S.; Bashir, E.; Shahab, B.; Rafiq, T. Discrete geochemical behavior of Sr and Ba in the groundwater of Southern Mor Range, Balochistan, a tracer for igneous and sedimentary rocks weathering and related environmental issues. *Appl. Geochem.* **2021**, *130*, 104996. [CrossRef]
29. Musgrove, M. The occurrence and distribution of strontium in U.S. groundwater. *Appl. Geochem.* **2021**, *126*, 104867. [CrossRef]
30. Plechacek, A.; Scott, S.R.; Gotkowitz, M.B.; Ginder-Vogel, M. Strontium and radium occurrence at the boundary of a confined aquifer system. *Appl. Geochem.* **2022**, *142*, 105332. [CrossRef]

31. Malov, A.I. *Groundwater of the South-East White Sea: Formation, Role in Geological Processes*; UB RAS: Yekaterinburg, Russia, 2003; p. 234. Available online: https://www.elibrary.ru/item.asp?id=1947446429 (accessed on 10 September 2023). (In Russian)
32. Salminen, R.; Chekushin, V.; Bogatyrev, I.; Fedotova, E.; Tomilina, O.; Zhdanova, L.; Tenhola, M.; Glavatskikh, S.; Gregorauskiene, V.; Kashulina, G.; et al. *Geochemical Atlas of the Eastern Barents Region*; Elsevier: Amsterdam, The Netherlands, 2004; p. 548.
33. USEPA. *Risk Assessment Guidance for Superfund. Volume I: Human Health Evaluation Manual (Part E, Supplemental Guidance for Dermal Risk Assessment)*; Final. EPA/540/R/99/005; U.S. Environmental Protection Agency: Washington, DC, USA, 2004.
34. Stankovsky, A.F.; Verichev, E.M.; Grib, V.P.; Dobeiko, I.P. Vendian of the southeastern White Sea. *Izv. Acad. Sci. USSR. Ser. Geol.* **1981**, *2*, 78–87. (In Russian)
35. Stankovsky, A.F.; Verichev, E.M.; Dobeiko, I.P. Vendian of the southeastern White Sea. In *Vendian System. Historical-Geological and Paleontological Substantiation. Vol. 2. Stratigraphy and Geological Processes*; Sokolov, B.S., Fedonkin, M.A., Eds.; Nauka: Moscow, Russia, 1985; pp. 67–76. (In Russian)
36. Turekian, K.K. *Chemistry of the Earth*; Holt, Rinehart and Winston Inc.: New York, NY, USA, 1972; p. 131.
37. Turekian, K.K.; Wedepohl, K.H. Distribution of the elements in some major units of the earth's crust. *Geol. Soc. Am. Bull.* **1961**, *72*, 175–192. [CrossRef]
38. Malov, A.I.; Sidkina, E.S.; Ershova, D.D.; Cherkasova, E.V.; Druzhinin, S.V. Time regularities of strontium concentration in drinking groundwater distant from the sea coast. *Env. Geochem. Health* **2023**, *45*, 8097–8118. [CrossRef] [PubMed]
39. Malov, A.I.; Sidkina, E.S.; Ryzhenko, B.N. Model of the Lomonosov diamond deposit as a water–rock system: Migration Species, Groundwater Saturation with Rock-Forming and Ore Minerals, and Ecological Assessment of Water Quality. *Geochem. Int.* **2017**, *55*, 1118–1130. [CrossRef]
40. Münnich, K.O. Messungen des ^{14}C-Gehaltes von hartem Grundwasser. *Naturwissenschaften* **1957**, *44*, 32–34. [CrossRef]
41. Münnich, K.O. Isotopendatierung von Grundwasser. *Naturwissenschaften* **1968**, *55*, 3–11. [CrossRef]
42. Ingerson, E.; Pearson, F.J. Estimation of age and rate of motion of groundwater by the ^{14}C method. In *Recent Researches in the Fields of Atmosphere, Hydrosphere and Nuclear Geochemistry*; Marusen: Tokyo, Japan, 1964; pp. 263–283.
43. Mook, W.G. On the reconstruction of the initial ^{14}C content of groundwater from the chemical and isotopic composition. In Proceedings of the Eighth International Conference on Radiocarbon Dating 1, Lower Hutt, New Zealand, 18–25 October 1972; Royal Society of New Zealand: Wellington, New Zealand, 1972; pp. 342–352.
44. Mook, W.G. The dissolution-exchange model for dating groundwater with ^{14}C. In *Interpretation of Environmental Isotope and Hydrochemical Data in Groundwater Hydrology*; IAEA: Vienna, Austria, 1976; pp. 213–225.
45. Han, L.-F.; Plummer, N. A review of single-sample-based models and other approaches for radiocarbon dating of dissolved inorganic carbon in groundwater. *Earth Sci. Rev.* **2016**, *152*, 119–142. [CrossRef]
46. Ferronsky, V.I.; Polyakov, V.A. Isotopes of the Earth's Hydrosphere. Springer: Amsterdam, The Netherlands, 2012. [CrossRef]
47. Vogel, J.C. Carbon-14 dating of groundwater. In Proceedings of the Symposium on Use of Isotopes in Hydrology, Vienna, Austria, 9–13 March 1970; IAEA: Vienna, Austria, 1970; pp. 225–237.
48. Reimer, P.J.; Austin, W.E.N.; Bard, E.; Bayliss, A.; Blackwell, P.G.; Ramsey, C.B.; Butzin, M.; Cheng, H.; Edwards, R.L.; Friedrich, M.; et al. The IntCal20 Northern Hemisphere radiocarbon age calibration curve (0–55 ka cal BP). *Radiocarbon* **2020**, *62*, 725–757. [CrossRef]
49. Stuiver, M.; Reimer, P.J.; Reimer, R.W. CALIB 8.2 [WWW Program]. Available online: http://calib.org (accessed on 16 February 2021).
50. Schoeller, H. Qualitative evaluation of groundwater resources. In *Methods and Techniques of Groundwater Investigation and Development*; UNESCO: Paris, France, 1967; Volume 33, pp. 44–52.
51. Schoeller, H. Geochemistry of groundwater. In *Groundwater Studies—An International Guide for Research and Practice*; UNESCO: Paris, France, 1977; Volume 15, pp. 1–18.
52. Steffanowski, J.; Banning, A. Uraniferous dolomite: A natural source of high groundwater uranium concentrations in northern Bavaria, Germany? *Env. Earth Sci.* **2017**, *76*, 508. [CrossRef]
53. Plummer, L.N. Defining reactions and mass transfer in part of the Floridan Aquifer. *Water Resour. Res.* **1977**, *13*, 801–812. [CrossRef]
54. Back, W.; Hanshaw, B.B.; Plummer, L.N.; Rahn, P.H.; Rightmere, C.T.; Rubin, M. Process and rate of dedolomitization: Mass transfer and ^{14}C dating in a regional carbonate aquifer. *Geol. Soc. Am. Bull.* **1983**, *94*, 1415–1429. [CrossRef]
55. Musgrove, M.; Banner, J.L. Controls on the spatial and temporal variability of vadose dripwater geochemistry: Edwards aquifer, central Texas. *Geochem. Cosmochim. Acta* **2004**, *68*, 1007–1020. [CrossRef]
56. Malov, A.I. Features of the formation of high strontium concentrations in drinking groundwater near sea coast. *Dokl. Earth Sci.* **2023**, *512*, 898–901. [CrossRef]
57. USEPA. *Health Effects Support Document for Strontium*; EPA 820-P-14-0012014; U.S. Environmental Protection Agency: Washington, DC, USA, 2014. Available online: www.epa.gov/safewater/ccl/pdf/Strontium.pdf (accessed on 10 September 2023).
58. USEPA. *Supplemental Guidance for Developing Soil Screening Levels for Superfund Sites*; OSWER 9355.4-24; U.S. Environmental Protection Agency: Washington, DC, USA, 2002.
59. Gerba, C.P. *Risk Assessment. Environmental and Pollution Science*, 3rd ed.; Elsevier: Amsterdam, The Netherlands, 2019; pp. 541–563. [CrossRef]

60. Means, B. Risk-Assessment Guidance for Superfund, Volume 1. In *Human Health Evaluation Manual, Part A*; Interim Report Final No. PB-90–155581/XAB; EPA-540/1–89/002; Environmental Protection Agency; Office of Solid Waste and Emergency Response: Washington, DC, USA, 1989. Available online: https://www.osti.gov/biblio/7037757 (accessed on 18 January 2022).
61. Ondayo, M.A.; Watts, M.J.; Hamilton, E.M.; Mitchell, C.; Mankelow, J.; Osano, O. Artisanal gold mining in Kakamega and Vihiga counties, Kenya: Potential human exposure and health risk. *Env. Geochem. Health* **2023**, *45*, 6543–6565. [CrossRef] [PubMed]
62. USEPA. Regional Screening Levels (RSLs). Calculator. Available online: https://epa-prgs.ornl.gov/cgi-bin/chemicals/csl_search (accessed on 3 August 2023).
63. Zhang, H.; Zhou, X.; Wang, L.; Wang, W.; Xu, J. Concentrations and potential health risks of strontium in drinking water from Xi'an, Northwest China. *Ecotoxicol. Environ. Saf.* **2018**, *164*, 181–188. [CrossRef] [PubMed]
64. Zimoch, I.; Łobos, E. Evaluation of health risk caused by chloroform in drinking water. *Desalin. Water Treat.* **2015**, *57*, 1027–1033. [CrossRef]